Biosynthesis of Pteridines. Stopped-Flow Kinetic Analysis of GTP Cyclohydrolase I[†]

Andreas Bracher,[‡] Nicholas Schramek, and Adelbert Bacher*

Lehrstuhl für Organische Chemie und Biochemie, Technische Universität München, Lichtenbergstrasse 4, D-85747 Garching, Germany

Received February 15, 2001; Revised Manuscript Received April 23, 2001

ABSTRACT: GTP cyclohydrolase I catalyzes a mechanistically complex ring expansion affording dihydroneopterin triphosphate from GTP. The inherently slow enzyme reaction was studied under single turnover conditions monitored by multiwavelength ultraviolet spectroscopy. The spectroscopic data array was subjected to singular value decomposition and thereby shown to comprise six significant linearly independent optical processes. The data were fitted to a model of six consecutive unimolecular reaction steps where the first was considered to be reversible. The rate-limiting step was shown to occur rather late in the reaction sequence.

GTP cyclohydrolases catalyze the first committed step in the biosynthetic pathways of tetrahydrofolate, tetrahydromethanopterin, tetrahydrobiopterin, flavocoenzymes, and various nucleoside analogues. Specifically, GTP cyclohydrolase I converts GTP (compound **1**, Figure 1) to dihydroneopterin triphosphate (compound **10**) (*1*, *2*) that serves as a biosynthetic precursor of tetrahydrofolate in plants and many microorganisms (*3*) and of tetrahydrobiopterin in animals (*4*, *5*).

The enzyme-catalyzed reaction involves the opening of the imidazole ring of GTP by hydrolysis of the C-8/N-9 bond, the release of formate by hydrolysis of the formamide bond of the intermediate, compound **4**, and an Amadori rearrangement of the carbohydrate side chain followed by ring closure under formation of the dihydropteridine chromophore (*1*, *2*, *6*−*10*).

The complex reaction sequence has been studied in some detail by biochemical and crystallographic analysis (*6*−*11*). An essential zinc ion complexed to two cysteine residues and one histidine residue was found to act as a Lewis acid involved in the nucleophilic attack of C-8 of GTP by water or a hydroxyl ion (*12*). The structure of the resulting formamide type intermediate, compound **4**, has been established by NMR[1] spectroscopy using multiply ^{13}C-labeled GTP as substrate (*13*). Enzymatic conversion of GTP to compound **4** has been shown to be reversible with an approximate equilibrium constant of 0.1 at pH 7.0 and 30 °C (*13*).

The downstream part of the enzyme-catalyzed reaction sequence is incompletely understood. The rearrangement of the carbohydrate side chain has been shown to involve a stereospecific protonation step (*8*).

Single turnover quenched-flow experiments with GTP cyclohydrolase I tentatively located the rate-limiting step to the terminal part of the reaction trajectory (*9*). A more detailed analysis of the complex reaction sequence is reported in this paper.

MATERIALS AND METHODS

Materials. 6,7-Dimethylpterin was purchased from Schircks Laboratories, Jona, Switzerland. 2-Amino-5-formylamino-6-ribosylamino-4(3*H*)-pyrimidinone 5′-triphosphate (compound **4**) was prepared as described earlier (*13*).

Enzyme Purification. Recombinant GTP cyclohydrolase I of *Escherichia coli* was prepared as described earlier (*8*).

Enzyme Assay. GTP cyclohydrolase I activity was measured by published procedures (*8*).

Single Turnover Experiments. Stopped-flow and quenched-flow experiments were performed with an SFM4/QS apparatus from Bio-Logic (Claix, France) equipped with a linear array of three mixers and four independent syringes. For stopped-flow measurements, the content of a 1.5 mm light path quartz cuvette behind the last mixer was monitored with a Tidas diode array spectrophotometer (200−610 nm) equipped with a 15 W deuterium lamp as light source (J&M Analytische Mess- und Regeltechnik, Aalen, Germany). The reaction buffer contained 10 mM Tris-HCl, pH 8.5, 100 mM KCl, and 2.5 mM EDTA. GTP cyclohydrolase I was used at a concentration of 6.6 mg mL^{-1} (equivalent to 267 μM subunits), and GTP was used at a concentration of 167 μM. At a total flow rate of 4 mL s^{-1}, the enzyme solution was mixed at 30 °C at a ratio of 1:1 with substrate solution. At that flow rate, the calculated dead time is 7.6 ms. During the reaction, spectra integrated over 48 ms were recorded at intervals of 100 ms.

Global Analysis of Data from Stopped-Flow Experiments. Prior to data analysis, the absorbance background caused by buffer and enzyme was removed by subtraction of a blank

[†]This work was supported by the Deutsche Forschungsgemeinschaft, the Fonds der Chemischen Industrie, and the Hans Fischer Gesellschaft.

* To whom correspondence should be addressed. Tel: +49-89-289-13360. Fax: +49-89-289-13363. E-mail: adelbert.bacher@ch.tum.de.

[‡] Present address: EMBL, 6 rue Jules Horowitz, F-38000 Grenoble, France.

[1] Abbreviations: HPLC, high-performance liquid chromatography; NMR, nuclear magnetic resonance.

10.1021/bi010322v CCC: $20.00
Published on Web 06/08/2001

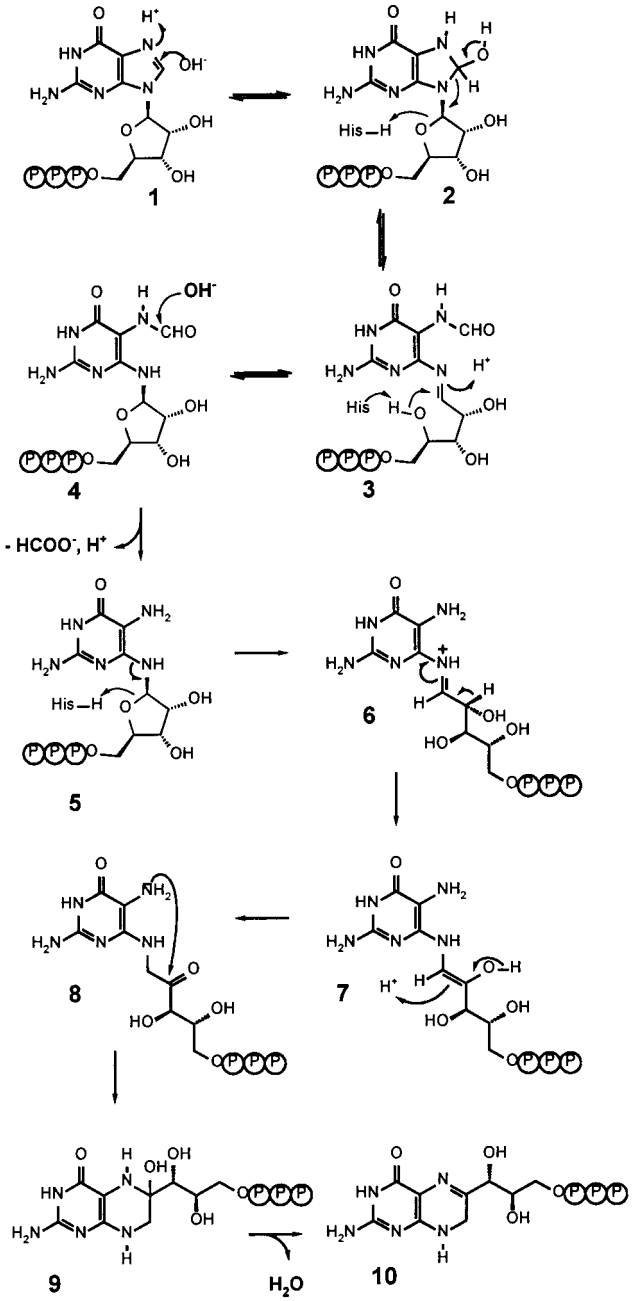

FIGURE 1: Hypothetical reaction mechanism of GTP cyclohydrolase I **(9)**.

data set obtained without addition of substrate. Data reduction and stronger weighting of early spectra were achieved by extracting 300 spectra on a pseudo-logarithmic time base from the difference data sets. These data sets were then analyzed using the program SPECFIT/32 3.0.12 (R. Binstead and A. Zuberbühler, Spectrum Software Associates, Marlbourough, MA).

Quenched-Flow Experiments. For quenched-flow experiments, the mixing apparatus was equipped with a computer-controlled valve instead of a cuvette. A delay loop of 230 μL nominal volume located between mixers 2 and 3 was filled with reactants at a total flow rate of 4 mL s^{-1}. At the times indicated, the reaction mixture in the delay loop was mixed at a 1:1 ratio at 30 °C with 1 M hydrochloric acid from syringe 4 at a flow rate of 4 mL s^{-1}. The effluent was stored at −70 °C for further analysis.

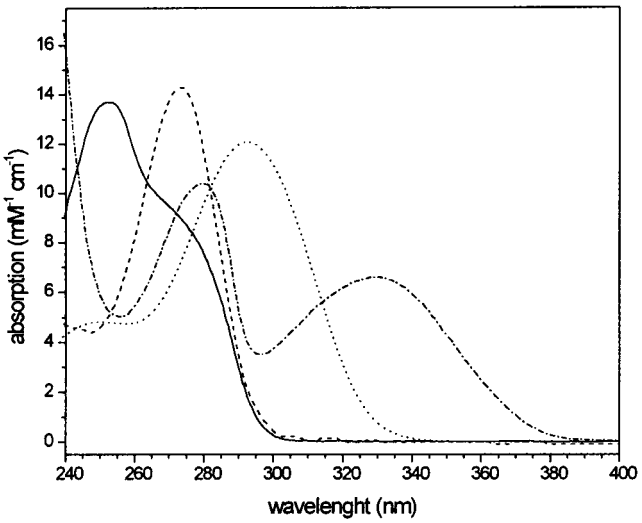

FIGURE 2: Ultraviolet spectra of compounds supposed to occur in the reaction trajectory of GTP cyclohydrolase I: (—) GTP (compound **1**); (- - -) 2-amino-5-formylamino-6-ribosylamino-4(3*H*)-pyrimidinone 5′-triphosphate (compound **4**); (···) 2,5-diamino-6-ribitylamino-4(3*H*)-pyrimidinone 5′-monophosphate obtained by treatment of GTP with GTP cyclohydrolase II (the corresponding triphosphate, compound **5**); (-·-) dihydroneopterin (the corresponding triphosphate, compound **10**).

Analysis of Reaction Mixtures. Acidic reaction mixtures from quenched-flow experiments were incubated at 90 °C for 5 min. After adjustment to pH 8.5 by addition of 1 M NaOH, butanedione was added to a final concentration of 0.5%. The mixtures were incubated at 90 °C for 1 h. 6,7-Dimethylpterin was determined by HPLC as described previously (*14*).

RESULTS

GTP cyclohydrolase I generates stoichiometric amounts of formate and dihydroneopterin triphosphate from GTP. Earlier quenched-flow studies had indicated that the rate of formation of formate exceeds that of dihydroneopterin triphosphate by approximately 1 order of magnitude (*9*).

The hypothetical reaction intermediates shown in Figure 1 are all characterized by heterocyclic chromophores suitable for optical detection. Specifically, the substrate, GTP, is characterized by an absorption maximum at 252 nm with a shoulder at 273 nm (Figure 2). The early reaction intermediate, 2-amino-5-formylamino-6-ribosylamino-4(3*H*)-pyrimidinone 5′-triphosphate (compound **4**), which has been identified earlier by NMR spectroscopy (*13*), has an absorption maximum at 273 nm. The enzyme product, dihydroneopterin triphosphate, is characterized by a broad absorption band at 330 nm and a more intense band centered at 280 nm. Figure 2 also shows the spectrum of 2,5-diamino-6-ribosylamino-4(3*H*)-pyrimidinone 5′-phosphate, the product of GTP cyclohydrolase II (*15*), which is likely to resemble closely the spectra of the hypothetical intermediates, compounds **5**, **7**, **8**, and **9**, which are all expected to have absorbency bands centered around 280 nm and should therefore be distinguishable from compounds **4** and **10**, respectively, on the basis of ultraviolet measurements.

In light of the negative cooperativity of GTP cyclohydrolase I (*16*), single turnover stopped-flow experiments were performed with an excess of enzyme subunits over proffered

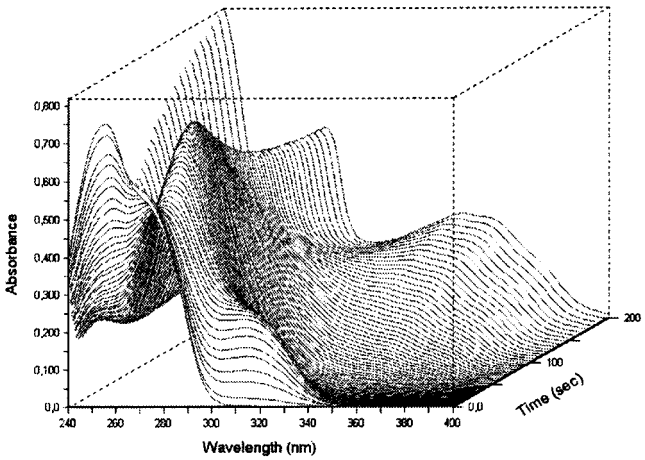

FIGURE 3: Optical spectra from a single turnover stopped-flow experiment.

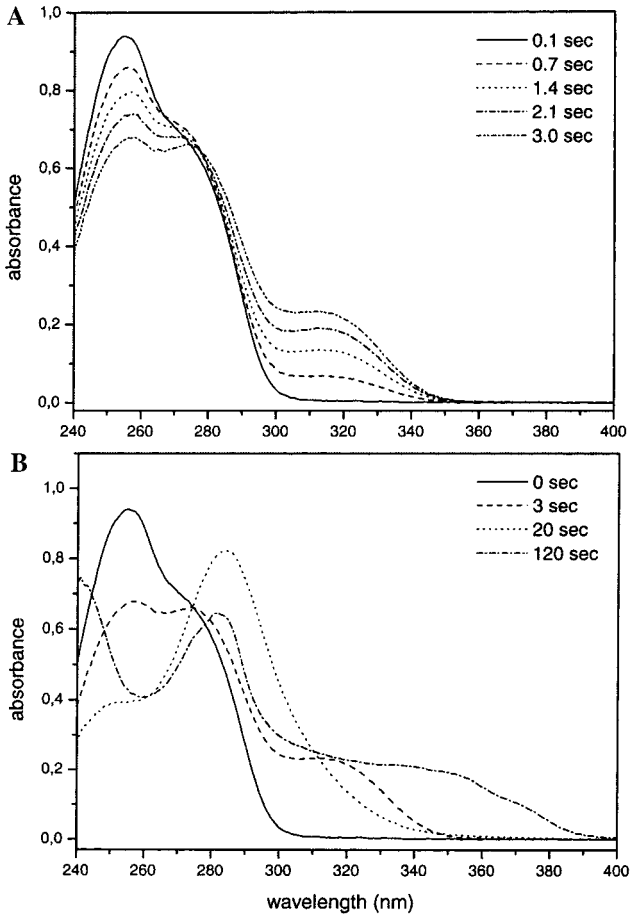

FIGURE 4: Ultraviolet spectra from the early phase (A) ant the later phase (B) of the single turnover experiment shown in Figure 3.

GTP. The reaction was monitored with an array photometer. A sequence of spectra is shown in Figure 3. In light of the complexity of the reaction sequence catalyzed by the enzyme, it is not surprising to observe a complex landscape with major absorbency changes occurring on a time scale extending from fractions of a second to several minutes.

Selected ultraviolet spectra from Figure 3 are shown in Figure 4. The initial phase of the reaction is characterized by a rapid, almost exponential decrease of the absorbency at 254 nm signaling the rapid consumption of GTP (Figure 5). Simultaneously, a broad band centered around 320 nm

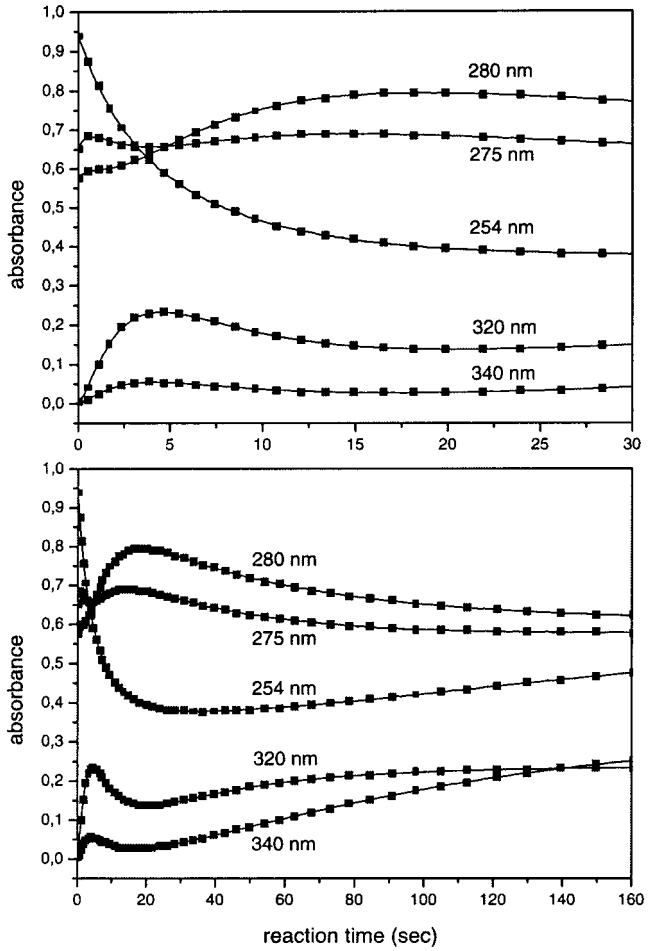

FIGURE 5: Absorbance changes observed during a single turnover stopped-flow experiment. Symbols represent experimental data from Figure 3. Solid lines represent the numerical simulation using the kinetic constants in Table 1.

reaches its maximum absorbency within approximately 4 s (Figures 4 and 5).

The spectra shown in Figure 4A almost intersect at 275 nm, thus suggesting a uniform reaction during the initial reaction time. However, on closer inspection, the absorbency at 275 nm is characterized by two maxima at 0.7 and 14.5 s and a minimum at 4 s, thus indicating the involvement of several different reaction steps occurring at different velocities in the early reaction phase (Figure 5).

The spectrum recorded after 20 s (Figure 4B) is similar to the spectrum of authentic 2,5-diamino-6-ribosylamino-4(3*H*)-pyrimidinone 5′-phosphate (i.e., the monophosphate analogue of the hypothetical intermediate, compound **5**) shown in Figure 2. It should be noted that the absorbency at 320 nm has decreased substantially by comparison with the spectrum obtained at 3 s. Obviously, the transient compound with a maximum at 320 nm has been consumed in the reaction progress.

The terminal part of the reaction sequence (extending from about 40 s to 4 min) is dominated by a slow but progressive increase of long-wavelength absorbency (Figure 5). However, there was concern that the spectroscopic data in this time period may be corrupted by photodecomposition of the enzyme product, dihydroneopterin triphosphate, occurring in the stopped-flow cuvette.

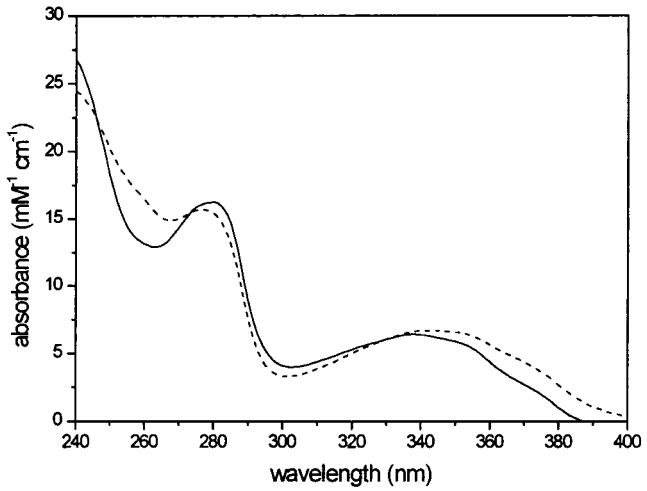

FIGURE 6: Photodecomposition of dihydroneopterin triphosphate under the experimental conditions of optically detected stopped-flow experiments: (—) spectrum of a reaction mixture incubated in the dark for 3 min; (- - -) same sample after irradiation in the stopped-flow cuvette for 3 min.

The suspected photochemical artifacts were directly confirmed by a reconstruction experiment performed as follows. The conversion of GTP to dihydroneopterin triphosphate was allowed to proceed to completion in the stopped-flow cell without light exposure. Spectroscopic observation of the reaction mixture was then initiated and showed the spectrum of dihydroneopterin triphosphate (Figure 6). Subsequently, ultraviolet illumination inherent in the continuous photometric observation was conductive to a red shift of the long-wavelength absorbency band (Figure 6) which may have involved a photodismutation of the enzyme product with formation of fully oxidized dihydroneopterin triphosphate as one of the reaction pathways.

For a more detailed analysis, the data set in Figure 3 was subjected to singular value decomposition using the program SPECFIT/32 3.0.12 (Spectrum Software Associates, Marlborough, MA), which indicated six linearly independent optical processes significantly above the noise floor. These data were numerically fitted to a kinetic model implicating five consecutive enzyme-catalyzed reaction steps followed by a sixth reaction step accounting for the artificial photodecomposition process.

$$A \underset{k_{-1}}{\overset{k_1}{\rightleftharpoons}} B \xrightarrow{k_2} C \xrightarrow{k_3} D \xrightarrow{k_4} E \xrightarrow{k_5} F \xrightarrow{k_6} G$$

Since earlier studies had documented the reversibility of the ring opening reaction affording the formamide type compound **4** from GTP (*13*), we introduced a reversible first reaction step. To overcome the resulting overparametrization, we included the known spectra of GTP (A) and 2-amino-5-formylamino-6-ribosylamino-4(3*H*)-pyrimidinone 5′-triphosphate (B) into our model. The other reaction steps were modeled as unimolecular forward reactions.

Only about 85% of proffered GTP have been shown to be converted to the enzyme product, compound **10**, in pre-steady-state quenched-flow experiments, even when significantly less than 1 equiv of GTP per enzyme subunit was used. The failure to convert all GTP to product in a single reaction cycle was attributed to partial zinc depletion of the enzyme during purification. An accurate value for the actual zinc content of the GTP cyclohydrolase I preparation used for stopped-flow experiments was not available. Several sets of calculations was performed with corrections for different fractions of residual GTP. In line with theoretical considerations, the corrections were conductive to minor changes of the rate constants but did not modify the general model. Figure 7 shows a kinetic model without correction for residual GTP.

The deconvoluted spectra of the molecular species A to G are shown in Figure 7A. The concentration curves for these molecular species are shown in Figure 7B. The quality of the fit can be estimated from the comparison between the experimental absorbency data with the sum of the fractional absorption contributions of components A to G according to the model using the kinetic constants shown in Table 1 (Figure 5).

The decay of the optical transient A is qualitatively similar to the consumption of GTP in earlier quenched-flow studies (*9*) although the latter suggested a somewhat more rapid decrease of GTP which may, however, be related to chemical instability under the conditions of acid quench. Our earlier quenched-flow study had also shown that the maximum concentration of the formamide intermediate does not exceed 10% of the starting concentration of GTP. This is well in line with the low intensity of the spectral component B (around 10% of starting GTP) at the time of its maximum concentration at 1.2 s.

The conversion of GTP to compound **4** had been shown earlier to be a reversible reaction by steady-state experiments with the H179A mutant as well as by quenched-flow experiments. The steady-state experiments had suggested a value of 0.1 for the equilibrium constant, but this value should be interpreted with caution, since the evaluation of the data was complicated by the isomerization of compound **4** affording four different stereoisomers (*13*). The quenched-flow experiments afforded values in the range of 0.07−0.45 for the equilibrium constant (*9*). The numerical analysis of the stopped-flow data reported in this paper suggests a value of 0.41. In light of the inherent methodical difficulties, the values from all three methods appear compatible.

The most conspicuous feature in the optical spectra from the stopped-flow experiments is the rapid formation of a species with an absorption maximum around 320 nm reaching a concentration maximum at 4 s (Figures 4 and 7B). Among the hypothetical reaction intermediates shown in Figure 1, the Schiff base, compound **6**, is the most plausible candidate for long wavelength around 320 nm due to the conjugation of the imine double bond with the quasiaromatic ring system.

The transient species characterized by the reconstructed spectrum D is characterized by an absorption maximum of 280 nm and by distinctly sigmoidal kinetics. The reconstructed spectrum is similar to the spectral envelope shown in Figure 4B (optical spectrum recorded at 20 s) and is the quantitatively dominant intermediary species observed in the course of the reaction. An absorption band with these characteristics appears plausible for the hypothetical intermediates **7** and **8**. Both compounds are substituted triamino-4(3*H*)-pyrimidinone type molecules devoid of side chain double bonds in resonance with the heterocyclic ring system.

Optical transient E represents a low-amplitude spectral process, which results in a maximum around 310 nm after

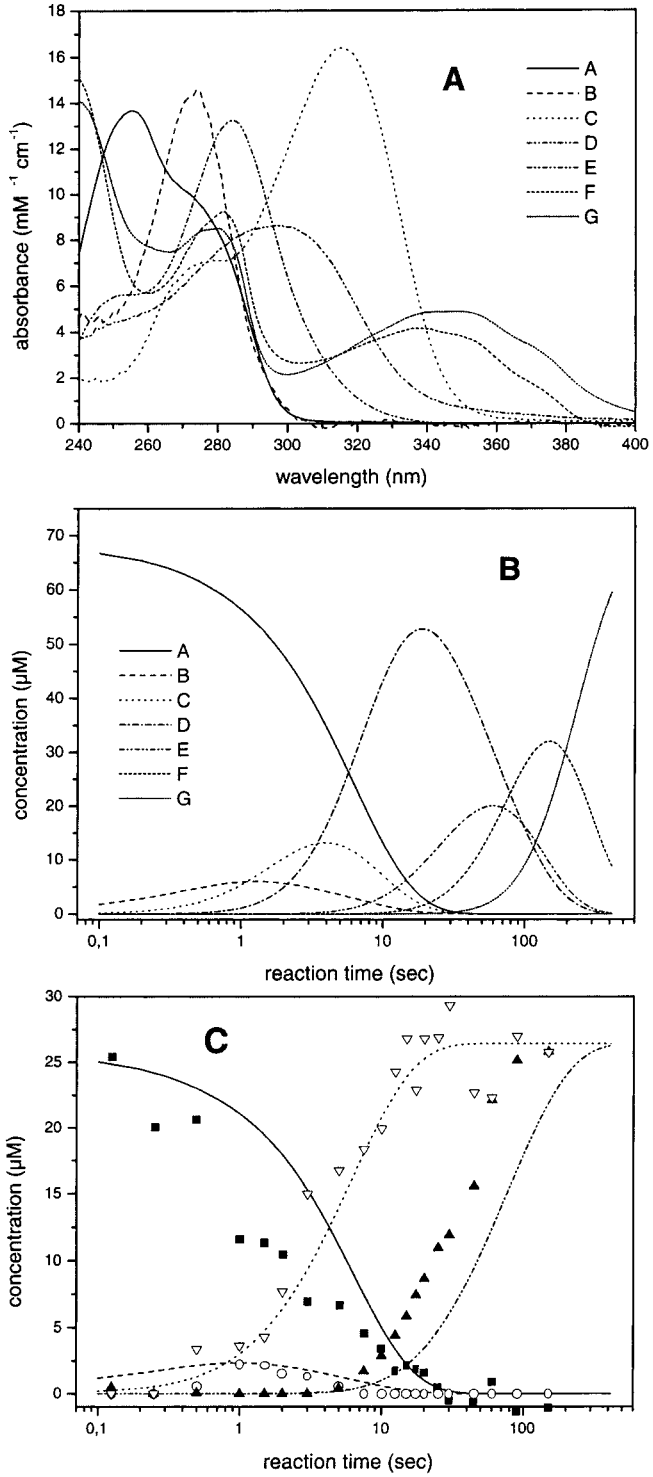

FIGURE 7: Numerical simulation of stopped-flow data: (A) reconstructed absorbance spectra of transient chromophores; (B) concentration of transient species; (C) comparison of single turnover stopped-flow (lines) and quenched-flow experiments (symbols). Symbols: (■) GTP (compound **1**); (○) 2-amino-5-formylamino-6-ribosylamino-4(3*H*)-pyrimidinone 5′-triphosphate (compound **4**); (▽) formate; (▲) dihydroneopterin triphosphate (compound **10**). Lines: (—) optical transient A; (- - -) optical transient B; (···) sum of optical transients C to G; (-·-) sum of optical transients E to G.

about 55 s. Since in numerical analysis the errors are distributed evenly among the parameters, low-amplitude spectral processes are expected to carry a higher error and corresponding spectra have to be interpreted with caution (Figure 7A). An association of transient E with the hydrated

Table 1: Kinetic Constants Obtained from Single Turnover Experiments

	rate constant (s^{-1})		rate constant (s^{-1})
k_1	0.229 ± 0.004	k_4	0.0161 ± 0.006
k_{-1}	0.559 ± 0.024	k_5	0.0245 ± 0.001
k_2	1.50 ± 0.03	k_6	0.0073 ± 0.0003
k_3	0.480 ± 0.006		

pteridine structure, compound **9**, is conceivable but can only be tentative. The reconstructed spectral components F and G show close similarity with the spectrum of dihydroneopterin triphosphate, respectively, the spectrum obtained after photodecomposition of dihydroneopterin triphosphate (Figure 6).

Whereas the correlation of optical transients with putative intermediates can only be tentative, it can be cross-checked by comparison with data from quenched flow (*9*). The consumption of GTP is qualitatively similar in the stopped-flow and quenched-flow experiments although GTP disappears more rapidly in the quenched-flow experiments by comparison with the stopped-flow experiment.

The stopped-flow and quenched-flow data for the formation and depletion of the formamide intermediate, compound **4**, are closely similar (Figure 7C). Both types of analysis indicate that the transient concentration of this intermediate does not exceed 10% of the total reactant concentration at any time during the reaction.

The concentration of formate must be equivalent to the sum of the concentrations of all heterocyclic products that are formed after the hydrolysis of compound **4** (i.e., to the sum of compounds **5**−**10** plus all heterocyclic compounds obtained by photooxidation) since all of the compounds must have been formed via compound **4** by the release of the formate moiety. Indeed, Figure 7C shows that the sum term of transients C to G corresponds closely to the concentration of formate determined by quenched-flow analysis (*9*).

To obtain additional data for the assignment of the optical transients, pre-steady-state reaction mixtures were quenched with hydrochloric acid, and the acidic mixtures were heated at 90 °C in order to cleave glycosidic bonds in all susceptible compounds. The resulting 2,5,6-triamino-4(3*H*)-pyrimidinone (compound **11**) was converted to 6,7-dimethylpterin (compound **13**), which was then detected by fluorescence-monitored HPLC. This analysis should detect the sum of all intermediates which are susceptible to hydrolytic release of the carbohydrate side chain under acidic conditions. Hence, it should represent the sum of compounds **3**−**6** and possibly compound **7** (Figure 8).

The sum of the concentrations of optical transients B to D as calculated from the stopped-flow data in Figure 7B is shown in Figure 9 (solid line) and is at least qualitatively similar to the result of the quenched-flow experiments shown in Figure 9 (symbols).

Compounds **8** and **9** are both expected to undergo ring closure and/or dehydration in the acidic mixture obtained by hydrochloric acid quench. In fact, the spontaneous reaction of 1-(2,5-diamino-1,6-dihydro-6-oxopyrimidine-4-ylamino)-1,5-dideoxy-L-*erythro*-pentulose has been used for preparative synthesis of dihydrobiopterin (*17*, *18*). Thus, the sum of the concentrations of optical transients E and F plus the concentrations of the artifactual photoproducts corresponding to the optical transient G should be equivalent to the amount

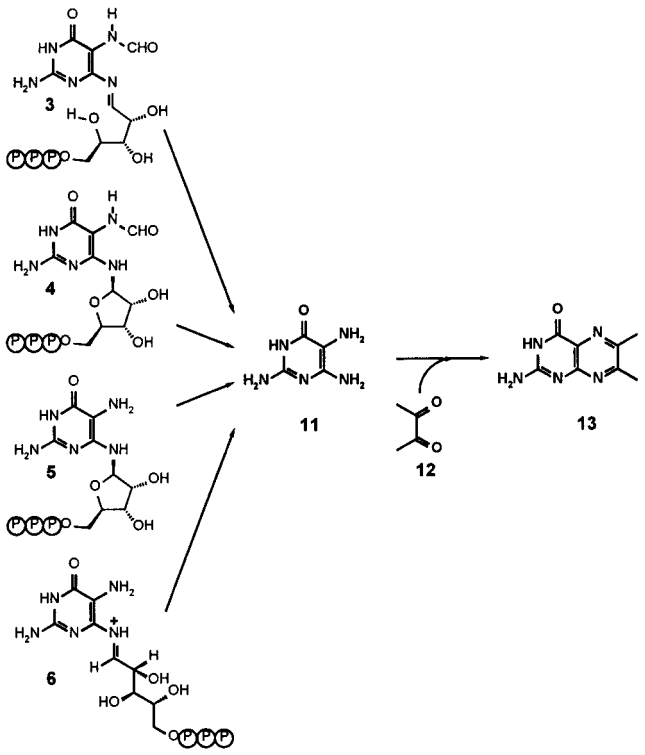

FIGURE 8: Comparison of single turnover stopped-flow and diacetyl quenched-flow experiments. Concentrations of 6,7-dimethylpterin (compound **13**) from quenched-flow experiments are indicated as symbols; the sum of intermediate B to D from stopped-flow experiments is represented as a solid line.

of dihydroneopterin triphosphate observed in quenched-flow experiments. It is obvious that the detection of the enzyme product, compound **10**, as diagnosed in the quenched-flow experiments precedes the curve derived from the stopped-flow data. As discussed in more detail below, this deviation could be easily explained if the closure of the pteridine ring occurs in the bulk solvent and is not enzyme catalyzed.

DISCUSSION

The following facts about the mechanism of GTP cyclohydrolase I have been established earlier. (i) The imidazole ring of GTP is hydrolytically opened between C-8 and N-9 (*10*). (ii) The rate for the liberation of formate exceeds that for the formation of the heterocyclic product, dihydroneopterin triphosphate, by approximately 1 order of magnitude (*9*). (iii) Utilization of the carbohydrate side chain of GTP involves the stereospecific introduction of a proton into the *pro*-7*R* position of the enzyme product (*8*).

Stopped-flow and quenched-flow analyses of the enzyme reaction are both faced with the problem that unequivocal

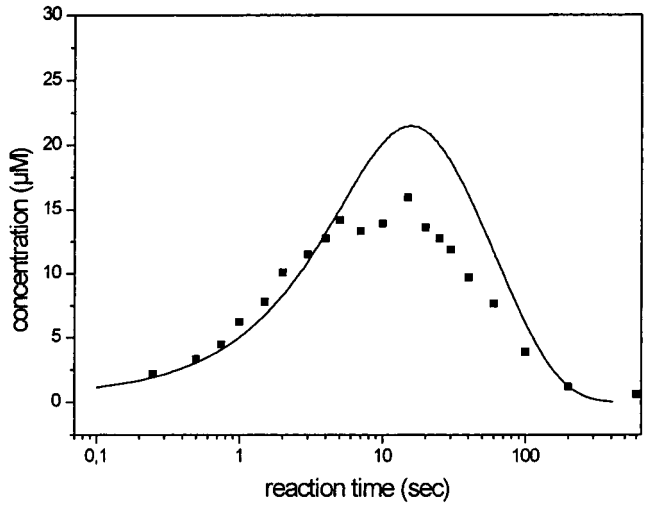

FIGURE 9: Expected reactions of putative reaction intermediates during acid hydrolysis followed by treatment with diacetyl (compound **12**). For details see Results.

assignment of observational parameters to specific intermediates in the complex reaction sequence is not possible. In quenched-flow experiments, different hypothetical intermediates can yield the same compound as a consequence of acid treatment. Specifically, the hypothetical intermediates **8** and **9** could be converted to compound **10** under the conditions of the acid quench. On the other hand, optical transients cannot be assigned unequivocally to specific reaction intermediates. Moreover, spectroscopic data as obtained in stopped-flow experiments suffer from the even more fundamental problem that optical transients are model dependent and every conceivable model accounting for the same number of linearly independent steps should yield comparable deviations from experimental data. Despite these caveats, both experimental approaches show that opening of the imidazole ring of GTP is rapid by comparison with the formation of dihydroneopterin triphosphate.

An Amadori rearrangement followed by ring closure is involved in the biosynthesis of tryptophan (Figure 10). The enzymatic conversion of *N*-(5′-phosphoribosyl)anthranilate (compound **14**) to 1-[(2-carboxyphenyl)amino]-1-deoxyribulose 5-phosphate (compound **16**) catalyzed by phosphoribosyl anthranilate isomerase has been studied by Hommel et al. (*19*), who showed that the formation of an enolamine intermediate (compound **15**) is rapid by comparison with the subsequent keto/enol tautomerization occurring as part of the Amadori rearrangement.

It is unknown whether the entire reaction sequence from GTP to dihydroneopterin triphosphate is actually enzyme catalyzed. Conceivably, the enzyme could release the Ama-

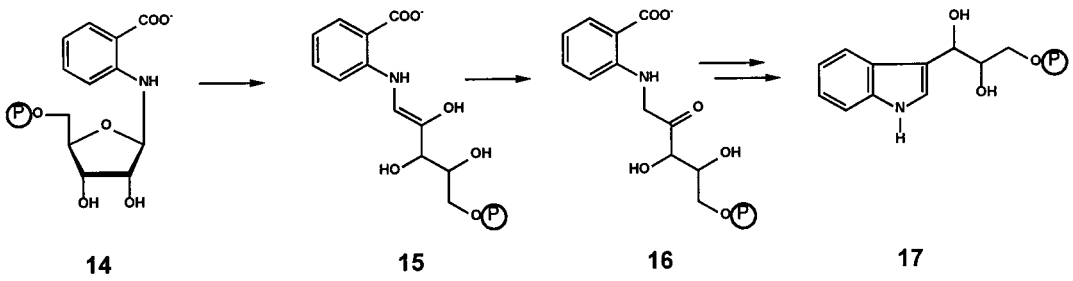

FIGURE 10: Reaction catalyzed by phosphoribosyl anthranilate isomerase (*19*).

dori product, compound **8**, which could subsequently undergo ring closure and dehydration in the bulk solvent. Both partial reactions could easily occur without catalysis under physiological conditions (*17*, *18*).

The formation of the dihydropteridine ring system requires a major conformational rearrangement of the reactant. The active sites of GTP cyclohydrolase I appear as relatively rigid cavities located at the respective interfaces of three adjacent subunits in the decameric protein. The triphosphate motif of the reactants is held in place by several basic amino acid residues inside the reaction cavity (*20*), and the position 2 amino group of GTP appears to be fixed by hydrogen bonds to glutamate 152. Formation of the pteridine ring system in situ would probably require a major conformational motion of the heterocyclic moiety in order to bring the position 5 amino group into a position adjacent to the carbonyl group of the carbohydrate side chain. Obviously, this would not arise if ring closure occurred in the bulk solvent rather than at the active site of the protein. The kinetic data obtained to date are unable to distinguish between these alternatives.

Even if the terminal reaction steps were to occur spontaneously in the bulk solvent rather than at the active site of the enzyme, the reaction sequence catalyzed by GTP cyclohydrolase I remains highly complex and involves the hydrolytic cleavage of two different CN bonds and the rearrangement of the carbohydrate moiety. Intuitively, the rearrangement of the carbohydrate moiety appears mechanistically straightforward by comparison with the hydrolytic opening of the chemically inert guanine ring system. The overall rate constant for the formation of 1-[(2-carboxyphenyl)amino]-1-deoxyribulose 5-phosphate (compound **16**, Figure 10) from *N*-(5′-phosphoribosyl)anthranilate (compound **14**) is approximately 3 orders of magnitude higher than the Amadori rearrangement catalyzed by GTP cyclohydrolase (*9*).

REFERENCES

1. Burg, A. W., and Brown, G. M. (1968) *J. Biol. Chem. 243*, 2349−2358.
2. Shiota, T., Palumbo, M. P., and Tsai, L. (1967) *J. Biol. Chem. 242*, 1961−1969.
3. Brown, G. M., and Williamson, J. M. (1987) in *Escherichia coli and Salmonella typhimurium* (Neidhardt, F. C., Ed.) pp 521−538, American Society for Microbiology, Washington, DC.
4. Tayeh, M. A., and Marletta, M. A. (1989) *J. Biol. Chem. 264*, 19654−19658.
5. Nichol, C. A., Smith, G. K., and Duch, D. S. (1985) *Annu. Rev. Biochem. 54*, 729−764.
6. Wolf, W. A., and Brown, G. M. (1969) *Biochim. Biophys. Acta 192*, 468−478.
7. Shiota, T., and Palumbo, M. P. (1965) *J. Biol. Chem. 240*, 4449−4453.
8. Bracher, A., Eisenreich, W., Schramek, N., Ritz, H., Götze, E., Herrmann, A., Gütlich, M., and Bacher, A. (1998) *J. Biol. Chem. 273*, 28132−28141.
9. Schramek, N., Bracher, A., and Bacher, A. (2001) *J. Biol. Chem. 276*, 2622−2626.
10. Shiota, T., Baugh, C. M., and Myrick, J. (1969) *Biochim. Biophys. Acta 192*, 205−210.
11. Nar, H., Huber, R., Meining, W., Schmid, C., Weinkauf, S., and Bacher, A. (1995) *Structure 3*, 459−466.
12. Auerbach, G., Herrmann, A., Bracher, A., Bader, G., Gütlich, M., Fischer, M., Neukamm, M., Garrido-Franco, M., Richardson, J., Nar, H., Huber, R., and Bacher, A. (2000) *Proc. Natl. Acad. Sci. U.S.A. 97*, 13567−13572.
13. Bracher, A., Fischer, M., Eisenreich, W., Ritz, H., Schramek, N., Boyle, P., Gentili, P., Huber, R., Nar, H., Auerbach, G., and Bacher, A. (1999) *J. Biol. Chem. 274*, 16727−16735.
14. Richter, G., Ritz, H., Katzenmeier, G., Volk, R., Kohnle, A., Lottspeich, F., Allendorf, D., and Bacher, A. (1993) *J. Bacteriol. 175*, 4045−4051.
15. Foor, F., and Brown, G. M. (1975) *J. Biol. Chem. 250*, 3545−3551.
16. Schoedon, G., Redweik, U., Frank, G., Cotton, R. G., and Blau, N. (1992) *Eur. J. Biochem. 210*, 561−568.
17. Andrews, K. J. M., Barber, W. E., and Tong, B. P. (1969) *J. Chem. Soc. 3*, 928−930.
18. Andrews, K. J. M., Barber, W. E., and Tong, B. P. (1968) *Chem. Commun. 6*, 120.
19. Hommel, U., Eberhard, M., and Kirschner, K. (1995) *Biochemistry 34*, 5429−5439.
20. Nar, H., Huber, R., Auerbach, G., Fischer, M., Hoesl, C., Ritz, H., Bracher, A., Meining, W., Eberhardt, S., and Bacher, A. (1995) *Proc. Natl. Acad. Sci. U.S.A. 92*, 12120−12125.

BI010322V